

Vanishing of the metal-insulator Peierls transition in pressurized BaVS₃

S. Bernu,¹ P. Fertey,² J.-P. Itié,² H. Berger,³ P. Foury-Leylekian,¹ and J.-P. Pouget¹

¹Laboratoire de Physique des Solides, Université Paris-Sud, CNRS-UMR 8502, 91405 Orsay Cedex, France

²Soleil Synchrotron, 91191 Gif-sur-Yvette Cedex, France

³Institut de Physique de la Matière Complexe, EPFL, 1015 Lausanne, Switzerland

(Received 2 February 2012; published 5 December 2012)

BaVS₃ presents a metal-to-insulator (MI) transition at ambient pressure due to the stabilization of a $2k_F$ commensurate charge density wave (CDW) Peierls ground state built on the dz^2 V orbitals. The MI transition vanishes under pressure at a quantum critical point (QCP) where the electronic properties exhibit a non-Fermi liquid behavior. In this paper, we determine the CDW phase diagram under pressure and show that it combines both the vanishing of the second-order Peierls transition and a commensurate-incommensurate first-order delocking transition of the $2k_F$ wave vector. We explain quantitatively the drop of the MI critical temperature by the decrease of the electron-hole pair lifetime of the CDW condensate due to an enhancement of the hybridization between the dz^2 and $e(t_{2g})$ levels of the V under pressure.

DOI: 10.1103/PhysRevB.86.235105

PACS number(s): 71.30.+h, 61.05.cp, 71.45.Lr

I. INTRODUCTION

An understanding of strongly correlated multiorbital electronic systems is one of the key issues needed to describe the physical properties of a wide range of novel solid state compounds.¹ The complex interplay of structural degrees of freedom with competing localized and itinerant electrons in the multiorbital case gives rise to unexpected physical phenomena and amazing properties such as unconventional superconductivity, giant magnetoresistance, and multiferroicity.² The large variety of competing ground states observed in these materials results from a balance between crystal phases with different charge, spin, lattice, and orbital orders. This subtle balance is strongly sensitive to external parameters such as the temperature, pressure, external fields, or chemical substitutions. Thus, the accurate determination of phase diagrams helps to understand the nature of the competing instabilities governing these complex systems. In this context, the transition metal sulfide BaVS₃, with both itinerant and localized electronic states together with a one-dimensional (1D) electronic anisotropy, is a model compound that displays, among its multiple instabilities, a metal-insulator (MI) transition that vanishes under pressure at a quantum critical point (QCP) at $P_{cr} \sim 2$ GPa.³⁻⁵ Furthermore, in the vicinity of P_{cr} , the restored metallic state behaves as a non-Fermi liquid (NFL).^{4,5} The NFL behavior is ascribed to strong interactions of fermions with collective excitations of the incipient ordered phase. In this paper, we propose that the MI transition associated with the Peierls ground state of BaVS₃ is destroyed by pressure, which induces a very efficient CDW depairing mechanism via a finite lifetime of the electron-hole pairs of the charge density wave (CDW) condensate, to lead finally to the QCP.

BaVS₃ is a bad metal,¹ the structure of which consists of a hexagonal packing of chains of face-sharing VS₆ octahedra running along the c axis, with two V atoms per unit cell. Its electronic structure contains three t_{2g} bands crossing the Fermi level: two narrow bands built on degenerate $e(t_{2g})$ orbitals and one quasi-1D dispersive band along c^* built with the dz^2 orbital; these bands are partly occupied by the $3d^1$ V electron. The localized $e(t_{2g})$ electrons are responsible for the magnetism of BaVS₃, and the delocalized dz^2 electrons

are responsible for its anisotropic metallic character.¹ At $T_S = 250$ K, BaVS₃ undergoes a Jahn-Teller transition, where V shifts away from the center of each octahedron to form zigzag chains. These V shifts lower the crystal symmetry from hexagonal to orthorhombic and lift the degeneracy of the $e(t_{2g})$ doublet into E_{g1} and E_{g2} components.¹ Then BaVS₃ undergoes a second-order MI transition at $T_{MI} = 70$ K and atmospheric pressure (P_{atm}). This transition corresponds to a Peierls transition below $T_P = T_{MI}$ that stabilizes a superstructure where the chain periodicity c is doubled.^{5,6} The satellite reflections, evidencing the symmetry breaking at the MI transition, are located at the commensurate (C), $(1, 0, \frac{1}{2})_O$ reduced reciprocal wave vector in the orthorhombic setting. The superstructure consists of a tetramerization of the V chains, with an out-of-phase order between first neighboring chains.⁶

The Peierls instability is driven by the formation below $T^* \sim 170$ K of $2k_F$ electron-hole pairs in the 1D dz^2 electronic subband⁶ (k_F being its Fermi wave vector). From the intrachain $2k_F = 1/2c^*$ component, one deduces⁶ that the CDW involves $\frac{1}{2} dz^2$ electrons per V. The remaining $\frac{1}{2}$ electrons per V, which account for the Curie constant of the localized magnetism of BaVS₃⁶, belong to the $e(t_{2g})$ states. The equal sharing of the $3d^1$ electron between dz^2 and $e(t_{2g})$ states has been explained by considering the interorbital Hund coupling.⁷ Below T_P , nonpaired $e(t_{2g})$ electrons remain magnetically active. Their spins develop antiferromagnetic (AF) correlations,⁸ which drive BaVS₃ into a triply incommensurate (IC) magnetic order below $T_N = 31$ K.⁹

II. EXPERIMENTAL DETAILS

The evolution of the Peierls transition under pressure ($P < 2$ GPa) has been measured from the diffraction of a single crystal placed in a diamond anvil cell (DAC). X-ray diffraction experiments were carried out using either a laboratory Rigaku Mo anode operating at 50 kV/150 mA or the synchrotron radiation at the ESRF ID20 beamline ($\lambda = 0.729$ Å) and at the SOLEIL CRISTAL beamline ($\lambda = 0.668$ Å). For the laboratory measurements, the diamonds of the anvil cell were cut with

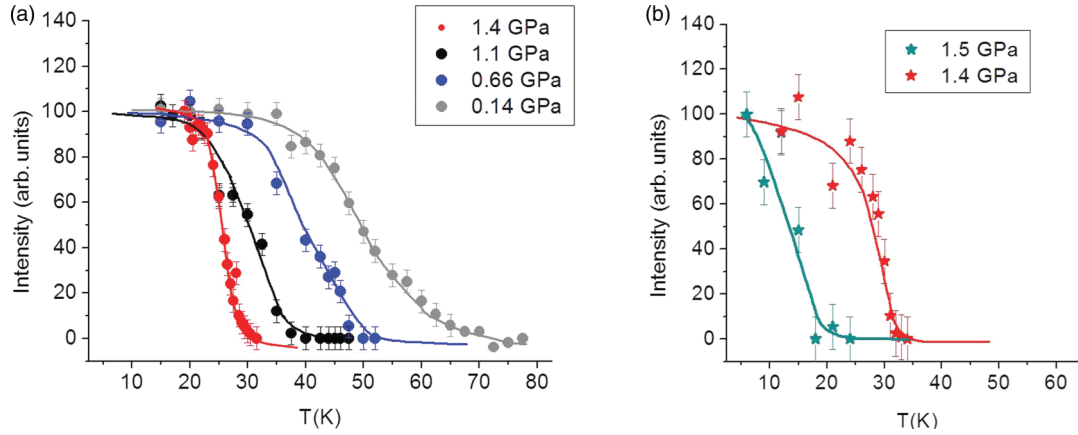


FIG. 1. (Color online) Thermal dependence of the integrated intensity of satellite reflections of BaVS₃ measured at different pressures and normalized at 100 at low temperature (the background has been subtracted from the signal). The extrapolated zero satellite intensity gives T_P reported in Fig. 2. The curves above 1.3 GPa have been obtained at the synchrotron Soleil facility. (a) Measurement obtained for CM satellite reflections and (b) for ICM satellite reflections.

a shape optimized to account for large single crystals without a too strong absorption of the Mo radiation used. Culet size was 1 mm, and the gasket was drilled with a 300 μm hole. The sample size was $200 \times 90 \times 90 \mu\text{m}^3$. A closed-circle He gas cryocooler was used to investigate the structural properties in the 10 K–300 K range. The detection was carried out with a standard NaI scintillator. For the synchrotron measurements, a specially designed membrane diamond anvil cell (MDAC) was used, allowing *in situ* variation of the pressure. The MDAC was inserted inside a home-made closed-circle He gas cryocooler operating from 6 K to 300 K (for the ESRF measurements, a liquid He cryostat was used in the 2–300 K temperature range). The sample size was $150 \times 100 \times 50 \mu\text{m}^3$. The crystal was previously oriented and mounted with the c^* axis perpendicular to the MDAC axis. A hybrid pixel detector XPAD (pixel size 130 μm) positioned at 700 mm from the sample was used during these measurements, giving a spatial resolution of $2.5 \times 10^{-3} \text{ \AA}^{-1}$ (half width at half maximum, HWHM). For all the measurements, the pressure transmission media was 4:1 methanol-ethanol. Pressure and temperature measurements were performed *in situ* using the ruby fluorescence technique with accuracy of ± 0.1 GPa and ± 0.5 K, respectively. The diffraction measurements were performed through the diamonds, and thanks to a 60° aperture, a large volume of the reciprocal space was accessible.

III. EXPERIMENTAL DETERMINATION OF THE (T, P) CDW-PEIERLS PHASE DIAGRAM

We followed the pressure behavior of several satellite reflections caused by the translational symmetry breaking at T_P . Figure 1 gives the thermal dependence of their normalized intensity at different pressures. The satellite intensity always drops continuously to zero at T_P , which means, in agreement with resistivity measurements,¹⁰ that the Peierls transition remains of second order, whatever the pressure. Figure 2 shows that T_P decreases nearly linearly with pressure until ~ 1.4 GPa, and then rapidly drops to zero. From our measurements, one estimates that the Peierls ground state vanishes around $P_{\text{cr}} \sim 1.8 \pm 0.1$ GPa, where no satellite reflection could be

detected above 2 K. T_P follows quite well the pressure dependence of T_{MI} identified from the maximum of the logarithmic derivative of the resistivity.^{4,10} In the linear regime, T_P and T_{MI} have an identical rate of decrease with pressure. The P_{cr} at which T_P vanishes appears to be 10% less than the value measured by transport measurements. This could result from possible differences in the P calibration or in the sample quality (defects and impurities have been shown to decrease T_P and to depress P_{cr} ¹⁹).

The $(1, 0, \frac{1}{2})_O$ reduced wave vector of the satellite reflections does not depend upon pressure below 1.35 GPa. Figure 3 compares H, K, L reciprocal scans around the $(2, 1, 2.5)_O$ superstructure and $(3, 1, 2)_O$ main Bragg reflections

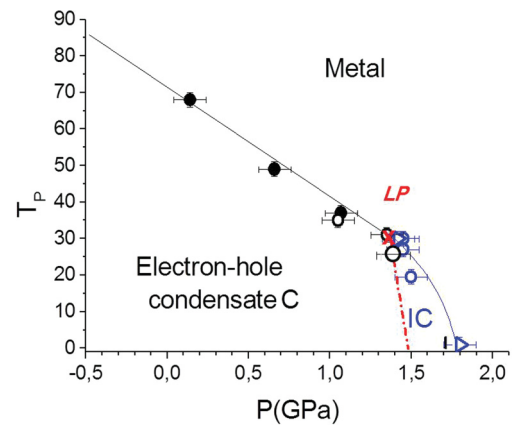


FIG. 2. (Color online) (T, P) phase diagram of the electron-hole condensate of BaVS₃. Full circles correspond to laboratory measurements, while the empty circles (Soleil) and triangles (ESRF) correspond to synchrotron measurements. The black symbols are related to the C transition, while the blue symbols correspond to the IC transition. The continuous curve is the fit of the pressure dependence of T_P by Eq. (1), where it has been assumed that α increases linearly with P . At $P = -0.5$ GPa: $\alpha = 0$ and $T_{P_0} = 86$ K; $\alpha \approx 1/4$ at P_{atm} and $\alpha = \alpha_c \approx 0.88$ at $P_{\text{cr}} \sim 1.8 \pm 0.1$ GPa. The first-order C-IC transition line is tentatively drawn, and the possible location of the Lifshitz point (LP, cross) is indicated.

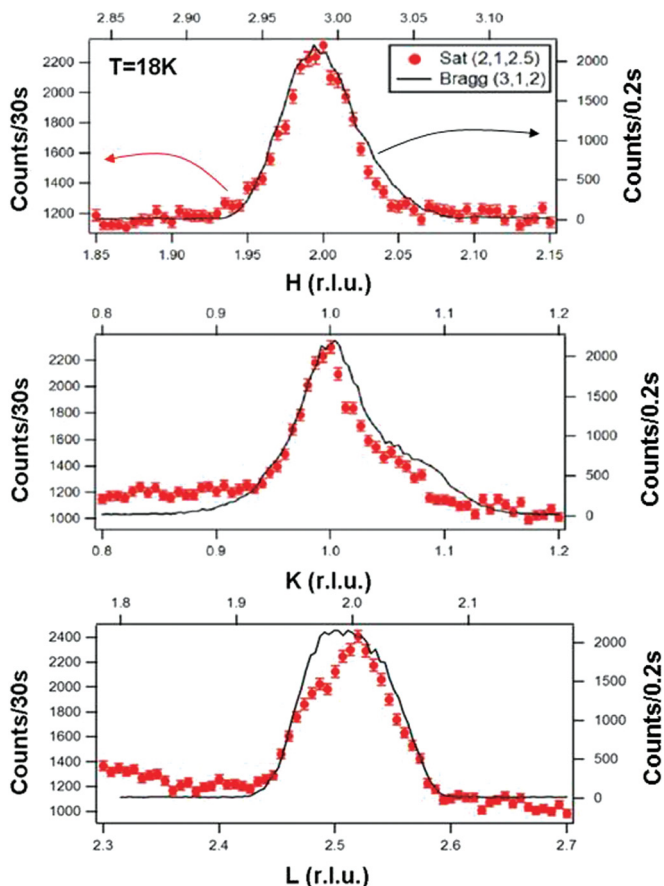


FIG. 3. (Color online) Superimposed H, K, L scans along a^* , b^* , and c^* directions (from top to bottom) for the $(2, 1, 2.5)_O$ satellite (points) and $(3, 1, 2)_O$ main Bragg (continuous line) reflections of BaVS_3 at 1.1 ± 0.1 GPa and 18 K. Note that the satellite reflection is 5×10^{-3} less intense than the main Bragg reflection.

at $P = 1.1 \pm 0.1$ GPa: (i) The satellite reflections are more than two orders of magnitude less intense than the main Bragg reflections, (ii) both kinds of reflection have the same width in all the reciprocal directions, which means that, at the scale of the experimental resolution, the long-range CDW order persists under pressure, and (iii) there is neither splitting nor broadening of the satellite reflections along c^* , which means that the $2k_F$ wave vector of the modulation remains pinned at the commensurate $1/2c^*$ value. This finding implies that in addition to the interorbital Hund coupling considered in Ref. 7, fourth-order umklapp processes (the dz^2 band is quarter filled) play a major role in promoting the equal sharing of the $3d^1$ V electron between the dz^2 and $e(t_{2g})$ orbitals.

At 1.4 GPa and above, a splitting of the satellite reflection wave vector of $(1, 0, 0.5 \pm \delta)_O$ is observed, as displayed in Fig. 4. While a^* and b^* satellite components remain commensurate with an accuracy of 10^{-3} rlu (reciprocal lattice units), the c^* component becomes IC. To accurately explore this C-IC transition, five measurements were performed between 1.35 GPa and 1.5 GPa. In this pressure range, the c^* component of the wave vector does not vary with the temperature at constant pressure. However, its deviation δ from $1/2c^*$ varies significantly with pressure: δ increases from 0.015 ± 0.001 rlu at 1.4 ± 0.1 GPa [Fig. 4(a)] to

0.024 ± 0.001 rlu at 1.5 ± 0.1 GPa [Fig. 4(b)]. Due to the difficulty of the measurement in the IC phase, only two pressure points were recorded, and the pressure variation of δ could not be accurately determined. It is also important to notice that measurements very close to P_{cr} are particularly difficult to perform from a technical point of view. Firstly, they require a very accurate determination of the pressure. Above P_{cr} , no superstructure reflections can be detected. Secondly, the intensity of the superstructure reflections is very weak and difficult to separate from the noise of the pressure cell. Finally, a cryostat with an optical window allowing the *in situ* measurement of the pressure limits the temperature range for the experimental investigations down to ~ 10 K.

In spite of the limited number of data, our measurements show that the critical $2k_F$ wave vector of the CDW instability of the dz^2 subband shifts from $1/2c^*$ to $(0.5 + \delta)c^*$ or $(0.5 - \delta)c^*$, indicating a significant deviation from the equal sharing of the $3d^1$ V electron between the dz^2 and $e(t_{2g})$ orbitals (diffraction measurements cannot indicate if $2k_F$ increases or decreases in the IC phase).

The diffraction pattern taken at 1.4 ± 0.1 GPa [Fig. 4(a)] also reveals a superimposition of C ($\delta=0$) and IC ($\delta \neq 0$) satellite reflections. This proves that BaVS_3 undergoes a discontinuous C-IC transition with a discontinuous jump of δ under pressure. At 1.4 GPa, the intensity of the C satellite reflections vanishes at 27.5 ± 0.5 K, while the intensity of the IC reflections vanishes at 31.5 ± 0.5 K (data shown in Fig. 1). At 1.5 GPa, the C satellite reflections are not detected down to 6 K, the lowest temperature reachable in this experiment. At this pressure, the IC reflections disappear at 19.5 ± 0.5 K. Thus, the first-order transition line that separates the C and IC phases, tentatively drawn in Fig. 2, is very steep. The merging of the first-order C-IC transition line with the T_P second-order transition line should occur at a so-called Lifshitz point (LP). As the LP is located on a second-order transition line, δ must deviate continuously from 0 when moving along this line. According to our measurements, the LP should be located at ~ 1.35 GPa and ~ 30 K.

Finally, the data of Fig. 4 show that the IC satellite reflections are broader along c^* (HWHM of $0.0058c^*$) than the C satellite reflections; these latter keep the experimental resolution of $0.0025c^*$. After correction by the experimental resolution, one estimates from the inverse HWHM of the satellite reflections that the IC order extends along c on about $\xi \sim 30c$.

IV. GENERAL DISCUSSION OF THE (T, P) PHASE DIAGRAM OF BaVS_3

A. Pressure dependence of the microscopic couplings

The observation under pressure of a C-IC transition and an unusual decay of the Peierls critical temperature T_P are the key results of this work, which should shed light on the BaVS_3 multiorbital electronic system. To understand these features, we must deepen the mechanism stabilizing the Peierls transition in BaVS_3 . The Peierls instability arises from the divergence at $2k_F$ of the electron-hole Lindhard function due to the nesting between the $+k_F$ and $-k_F$ points of the 1D dz^2 Fermi surface (FS).¹¹ This divergence, when coupled to the lattice degrees of freedom, gives rise to the observed

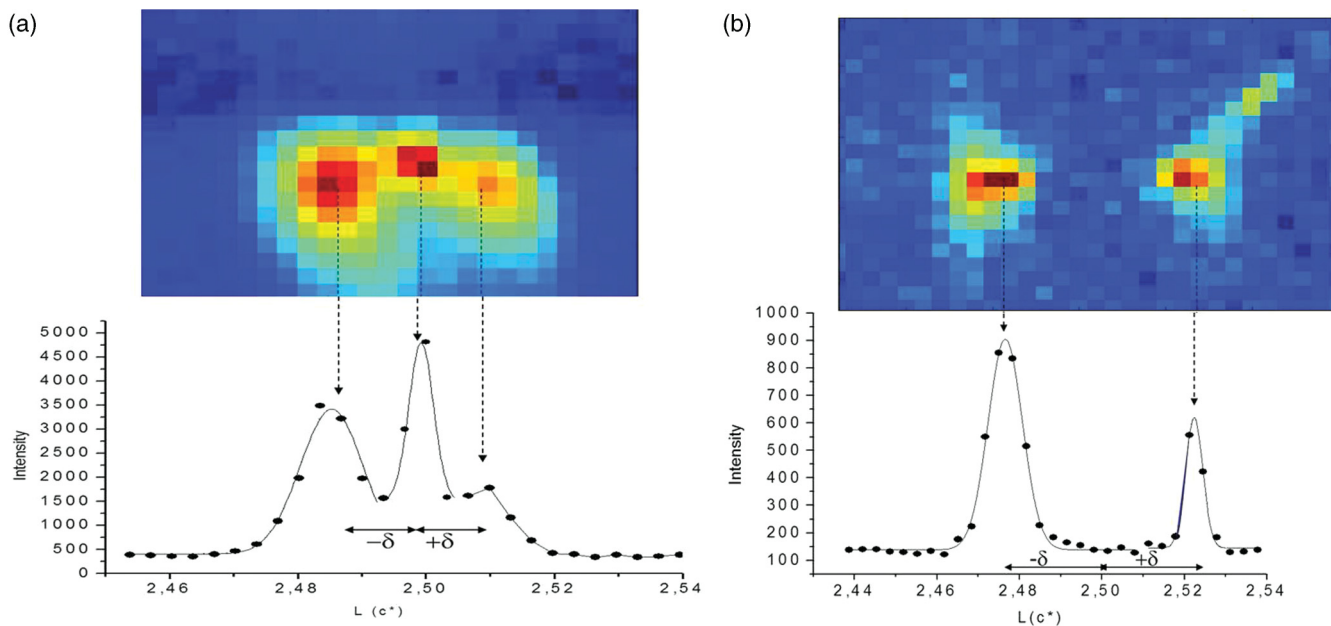


FIG. 4. (Color online) Reconstructed x-ray patterns showing the $\pm \delta$ split of the $(-2 -1 2.5)$ satellite reflection along c^* at 1.4 ± 0.1 GPa and 12 K (a) and 1.5 ± 0.1 GPa and 6 K (b). (For both measurements, the temperature is well below $T_P[P]$.) The lower part of the figure gives scans along c^* through the satellite reflections fitted (continuous lines) with Gaussian profiles. Note that (a) shows a superimposition of IC and C reflections. c^* direction is horizontal, and $a^* + b^*$ direction is vertical.

1D $2k_F$ CDW x-ray diffuse scattering fluctuations, which develop below T^* in BaVS_3 .⁶ These 1D CDW fluctuations give rise to a pseudogap in the density of state,¹¹ which affects the electronic properties of BaVS_3 below T^* ,¹² and especially the rate of decrease of its metallic conductivity. Then 1D CDW fluctuations begin to couple three dimensionally due to interchain transverse coupling below ~ 80 K.⁶ Finally the short-range CDW order diverges into a 3D long-range CDW order at $T_P = 70$ K. Several arguments developed elsewhere^{12,13} prove that the transverse coupling between 1D CDWs in the BaVS_3 system is driven by Coulomb coupling and not by the FS nesting. It is expected that the Coulomb coupling increases with pressure due to the decrease of the first neighbor interchain distance (by the combined effect of the decrease of lattice parameters¹⁴ and of the increase of the orthorhombic distortion¹⁵). Thus, the drop of T_P with pressure is unlikely due to the decrease of the interchain coupling.

Here, in agreement with conductivity measurements showing a reduction of the 1D pseudogap regime under pressure,⁴ we suggest that the effect of pressure is to smooth the $2k_F$ divergence of the Lindhard function of the 1D dz^2 electronic subsystem. More precisely, the linear decrease of T_P with modest pressure and its abrupt vanishing just below P_{cr} could be related to a very efficient electron-hole depairing mechanism associated with the electron-hole finite lifetime τ , which smoothes the divergence of the Lindhard function. More quantitatively, considering the electron-hole pair breaking parameter, $\alpha = \hbar/2\tau k_B T_{P_0}$, and the mean-field approximation, T_P decreases when α increases as:¹⁶

$$\text{Ln}(T_{P_0}/T_P) = \psi(1/2 + \alpha T_{P_0}/2\pi T_P) - \psi(1/2), \quad (1)$$

where $\psi(x)$ is the digamma function, and T_{P_0} is the Peierls transition temperature in absence of pair breaking. For small α ,

one gets a linear decrease of T_P ($T_P/T_{P_0} = 1 - \pi\alpha/4$), which well accounts for the experimental data of Fig. 2, below 1.4 GPa (if one assumes that α increases linearly with pressure). If the FS broadening due to this lifetime effect, \hbar/τ , is larger than half the mean field Peierls gap ($= 1.76 k_B T_{P_0}$), the Peierls transition is suppressed. This occurs for $\alpha > \alpha_c = 0.88$. As shown in Fig. 2, Eq. (1) fits nicely the total pressure dependence of T_P if one fixes $T_{P_0} \approx 86$ K and $\alpha \approx 1/4$ at P_{atm} .

It is interesting to notice that, at P_{atm} , $\alpha = 1/4$ leads to $\hbar/\tau \approx 44$ K. The value for \hbar/τ is close to the energy of the $2k_F$ critical phonon mode of BaVS_3 , $\hbar\Omega_{2k_F} \approx 50$ K.¹⁷ This means, with the condition $\Omega_{2k_F}\tau \sim 1$, that the Peierls lattice dynamics of BaVS_3 should be at the crossover between the adiabatic regime (where for $\Omega_{2k_F}\tau < 1$ the Peierls lattice instability is triggered by the softening of a $2k_F$ Kohn anomaly) and the nonadiabatic regime (where for $\Omega_{2k_F}\tau > 1$ the Peierls lattice instability is due to the critical growth of a $2k_F$ quasielastic response without phonon softening).¹⁸ The crossover condition $\Omega_{2k_F}\tau \sim 1$ thus deduced by our τ estimation is corroborated by the experimental observation¹⁷ of only a weak softening of the $2k_F$ critical phonon mode at T_P .

B. The electron-hole pair lifetime

Let us discuss more precisely the origin of the finite electron-hole pair lifetime τ in BaVS_3 . The CDW ground state is a condensate of electron ($+/-k_F$)-hole ($-/+k_F$) pairs as schematically illustrated in Fig. 5(a). For a conventional Peierls transition, pair breaking is due, as illustrated in Figure 5(b), to the backscattering (from $+k_F$ to $-k_F$ in the bottom of this figure) of electrons on the impurity potential, which, by changing the sign of their k_F wave vector, cannot any more pair with holes of opposite wave vector. This leads to a decrease

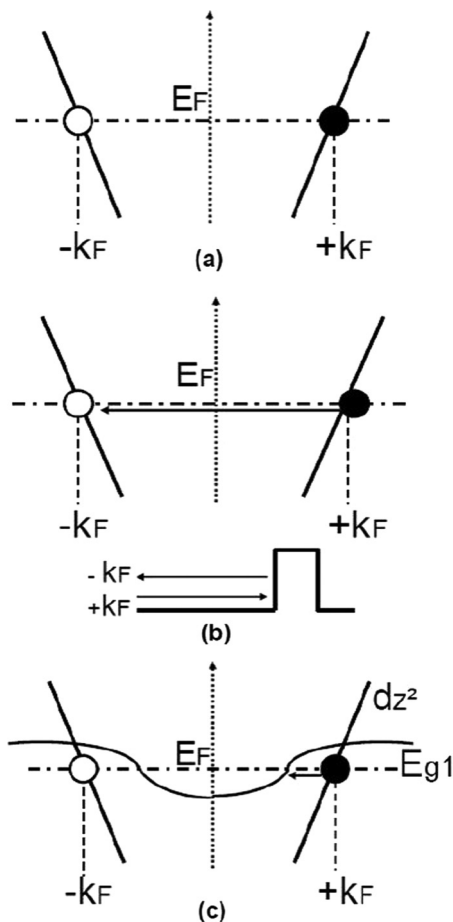


FIG. 5. (a) Schematic representation of a $(+k_F)$ electron- $(-k_F)$ hole pair forming the $2k_F$ CDW condensate. (b) $-2k_F$ backscattering of a $(+k_F)$ electron on the impurity potential (lower part of the figure), which breaks, by the change of sign of its k_F momentum, the electron-hole pairing. (c) Transition of a $(+k_F)$ electron from the dz^2 1D band to the Eg_1 state, which breaks the dz^2 electron-hole pairing.

of T_P when α increases with the amount of disorder. A linear decrease of T_P with the number of point defects is observed in $BaVS_3$ irradiated by fast electrons.¹⁹ In this case, the disorder is due to irradiation defects. A decrease of T_P is also observed with x increasing in the $Ba_{1-x}Sr_xVS_3$ solid solution for $x \leq 10\%$ ^{20,21} (for larger x values, an IC short-range order attributed to a charge ordering is observed). In this solid solution, the disorder is due to lattice deformations (size effect) induced by the isoelectronic Sr/Ba substitution. In these two systems, the C Peierls transition is kept while T_P decreases by less than 10 K. In “pure” $BaVS_3$, there is no reason that the pair-breaking process due to a residual disorder should be more strongly enhanced by the pressure. Thus, we propose a new pair-breaking process due to the presence of several orbital degrees of freedom at the Fermi level revealed by band structure calculations.⁷ As only the carriers of the dz^2 subband contribute to the CDW electron-hole pairing, a transition from the dz^2 to the $e(t_{2g})$ orbital states will destroy the pairing as illustrated in Fig. 5(c). This process requires the existence of an hybridization between the dz^2 and $e(t_{2g})$ orbital. Indeed, a hybridization between the dz^2 and the Eg_1 component of $e(t_{2g})$ is set by the orthorhombic distortion.^{22,23} It is expected

that this hybridization will be enhanced under pressure with the increase of the orthorhombic distortion.¹⁵ This will lead to an enhancement of the pair-breaking parameter α , and thus to a decrease of τ .

In this picture, if the pair-breaking parameter α exceeds $\alpha_c = 0.88$ (i.e., if the electron-hole lifetime τ is too short), the Peierls distortion vanishes. This situation should occur in the isostructural $BaVSe_3$ compound. This compound presents a dz^2 quasi-1D band structure as in $BaVS_3$ ²⁴ but does not undergo a Peierls MI transition.²⁵ However, transport measurements show that there is considerable similarity between the ambient-pressure $BaVSe_3$ and the high-pressure ($P > P_{cr}$) $BaVS_3$.²⁵ $BaVSe_3$ exhibits a higher orthorhombic transition ($T_S \sim 300$ K²⁶) than $BaVS_3$ below P_{cr} ($T_S < 270$ K¹⁵) and a stronger hybridization between dz^2 and $e(t_{2g})$ orbitals.²⁴ In that case, we suspect that the possible $2k_F$ dz^2 CDW instability cannot develop in $BaVSe_3$ due to the too short electron-hole lifetime τ (i.e., stronger hybridization between dz^2 and $e(t_{2g})$ orbitals).

C. General aspects of the phase diagram

In the mean-field scenario of the Peierls transition, an external parameter changing the band filling is expected to induce a delocking C-IC transition (at a LP) when the gain of C umklapp stabilizing energy is balanced by the loss of electronic energy due to the misfit δc^* between the C and IC $2k_F$ wave vectors (the Lindhard function diverges at the $2k_F$ wave vector associated with the band filling).^{27,28} This scenario predicts in the function of this external parameter a decrease of T_P towards the C phase, followed by a saturation in the rate of decrease of T_P towards the IC phase. It leads to an inflection point in the rate of decrease of T_P at the LP, which contradicts the observation of a rapid drop of T_P beyond the LP in $BaVS_3$.²⁹ Note that this calculation of the Peierls phase diagram in the presence of umklapp scattering ignores the electron-hole pair-breaking effect previously considered.

In principle, near the C-IC transition, the IC modulation should be described by a soliton lattice. Such a lattice is made of commensurate domains separated by phase shifts of $2\pi/p$ between two neighboring C domains (here $p = 4$ because the commensurability is set by a fourth-order umklapp potential). Each phase shift of $2\pi/p$ is achieved by a discommensuration. Two neighboring discommensurations are separated by a period l related to δc^* by $l = (2\pi/p\delta c^*)$. Our data give $l = 10c$ at 1.5 GPa. However in the case of $BaVS_3$, where the IC order extends on $\xi \sim 30c$, the soliton lattice, if it exists, should be quite disordered, because ξ is less than the total period pl (i.e., $4l \sim 40c$), achieving a phase shift of 2π . In the presence of a disorder, the soliton lattice will not be regular enough to give rise to harmonics of modulation.³¹ Indeed, such harmonics have not been detected in the diffraction pattern.

Interestingly, if discommensurations are present, even locally, they should bear the excess or defect of charge with respect to the quarter filling of the dz^2 band. A local order of discommensurations implies a local order of these additional charges. However, between the LP and P_{cr} , the presence of discommensurations should induce peculiar features in the transport properties and optical spectra of $BaVS_3$. Additional studies are required to detect their eventual presence.

At P_{atm} , there is an orbital order between the d_{z^2} and $e(t_{2g})$ electrons.³³ Beyond the LP, the spatial distribution of additional d_{z^2} charges in the IC modulation should also react to the orbital order and modify the magnetic coupling between the $e(t_{2g})$ spins (for which the average number per site will be incommensurate because there is one electron per V to share between the d_{z^2} and $e(t_{2g})$ states). Note at this point that our description of the ground state as a soliton lattice is oversimplified, taking into account only the spatial modulation of the d_{z^2} order parameter and ignoring the presence of the $e(t_{2g})$ degrees of freedom.

The correlation between the vanishing of T_P and the development of an IC CDW phase below the LP thus requires further investigations. A full understanding should rely on the consideration of the global phase diagram of BaVS₃, which is more complex than the one shown in Fig. 2 and which only focuses on the CDW-Peierls transition of the d_{z^2} electrons. The main reason is that the LP is close to the merging point of the T_P and T_N lines.³⁴ Thus, close to the LP, and contrary to BaVS₃ at low P , the $e(t_{2g})$ magnetic order (if it still persists) will not be established inside a well-defined Peierls superstructure (i.e., a sublattice of d_{z^2} singlet pairs). In this situation and in the presence of strongly fluctuating d_{z^2} pairing, the exchange coupling path between the spins of the $e(t_{2g})$ electrons will be certainly modified with respect to the one setting the AF-like order at P_{atm} .^{9,12} The correlations between critical fluctuations tending to promote local formation of d_{z^2} electron-hole singlet pairs and $e(t_{2g})$ magnetic order should be the key ingredient to construct the phase diagram between the LP and P_{cr} . In this respect, magneto-transport measurements¹⁰ show that the magnetic field curiously broadens the MI transition in the vicinity of P_{cr} . This proves that charge and spin degrees

of freedom are intimately connected in that pressure range. Furthermore, the mixing of spin and charge fluctuations should enhance the d_{z^2} electron-hole depairing and thus depress T_P . This would modify the behavior predicted by Eq. (1) and help to stabilize the QCP.

V. CONCLUSION

In conclusion, we have shown that below 1.4 GPa, the critical temperature of the MI transition of BaVS₃ decreases linearly with pressure while the CDW wave vector remains commensurate. A mechanism of electron-hole pair breaking well accounts for this $T_P(P)$ dependence. The origin of the pair breaking has been ascribed to a strengthening hybridization between the d_{z^2} and the $e(t_{2g})$ states, which kills the CDW collective state observed at P_{atm} . At higher pressures, an unexpected delocking C-IC transition is observed. This could lead to a possible formation of a soliton lattice incorporating the excess or defect of d_{z^2} charge. The theoretical understanding of this behavior, and particularly the abrupt vanishing of T_P with pressure towards a QCP, is actually totally missing due to the competing instabilities arising from the multiband nature of this system. Our determination of the (P, T) phase diagram of the quasi-1D strongly correlated compound BaVS₃ will help ongoing efforts for further theoretical investigations of multi-orbital electronic systems taking into account the charge, spin, orbital, and lattice degrees of freedom on the same footing.

ACKNOWLEDGMENT

N. Barišić is thanked for illuminating discussions.

¹M. Imada, A. Fujimori, and Y. Tokura, *Rev. Mod. Phys.* **70**, 1039 (1998).

²S.-W. Cheong and M. Mostovoy, *Nat. Mater.* **6**, 13 (2007).

³S. Sachdev, *Quantum Phase Transitions*, 2nd ed. (Cambridge University Press, Cambridge, UK, 2011).

⁴L. Forró, R. Gaál, H. Berger, P. Fazekas, K. Penc, I. Kézsmárki, and G. Mihály, *Phys. Rev. Lett.* **85**, 1938 (2000).

⁵I. Kézsmárki, G. Mihály, R. Gaál, N. Barišić, H. Berger, L. Forró, C. C. Homes, and L. Mihály, *Phys. Rev. B* **71**, 193103 (2005).

⁶S. Fagot, P. Foury-Leylejian, S. Ravy, J.-P. Pouget, and H. Berger, *Phys. Rev. Lett.* **90**, 196401 (2003).

⁷F. Lechermann, S. Biermann, and A. Georges, *Phys. Rev. Lett.* **94**, 166402 (2005).

⁸H. Nakamura, T. Yamasaki, S. Giri, H. Imai, M. Shiga, K. Kojima, M. Nishi, K. Kakurai, and N. Metoki, *J. Phys. Soc. Jpn.* **69**, 2763 (2000).

⁹P. Leininger, V. Ilakovac, Y. Joly, E. Schierle, E. Weschke, O. Bunau, H. Berger, J.-P. Pouget, and P. Foury-Leylejian, *Phys. Rev. Lett.* **106**, 167203 (2011).

¹⁰P. Fazekas, N. Barišić, I. Kézsmárki, L. Demkó, H. Berger, L. Forró, and G. Mihály, *Phys. Rev. B* **75**, 035128 (2007).

¹¹D. Jérôme and H. J. Schulz, *Adv. Phys.* **31**, 299 (1982).

¹²P. Foury-Leylejian, P. Leininger, V. Ilakovac, Y. Joly, S. Bernu, S. Fagot, and J.-P. Pouget, *Physica B* **407**, 1692 (2012).

¹³If a magnetic field, H_{\perp} , is applied perpendicularly to the chain direction, it is predicted that T_P caused by the nesting of a warped Fermi surface should increase because H_{\perp} renders the electron trajectory more 1D. In BaVS₃, the opposite effect is observed: T_P decreases with increasing H_{\perp} , both at P_{amb} and under P (see Ref. 12 and references therein for a discussion on this particular aspect).

¹⁴A. B. Garg, V. Vijayakumar, A. Choudhury, and H. D. Hochheimer, *Z. Naturforsch. B* **63**, 661 (2008).

¹⁵Here we assume that the local amplitude of the orthorhombic distortion scales with T_S . Only T_S , which increases from 250 K at P_{atm} to 270 K at 1.95 ± 0.1 GPa, has been determined under pressure.¹²

¹⁶B. R. Patton and L. J. Sham, *Phys. Rev. Lett.* **33**, 638 (1974).

¹⁷Y. Tanaka, J. Sutter, A. Baron, S. Tsutsui, and H. Nakamura, *Spring-8 Experimental Report 2005A0157-ND3d*, p. 160 (unpublished).

¹⁸The influence of the adiabatic-nonadiabatic crossover on the dynamics of the $2k_F$ critical phonon mode has been studied for the spin-Peierls chain by C. Gros and R. Werner, *Phys. Rev. B* **58**, 14677(R) (1998). In this reference, τ is the thermal lifetime $\hbar/\pi k_B T$, but the argument holds whatever the origin of τ . The change of nature of the $2k_F$ critical dynamics at this crossover is well illustrated in figure 4 of J.-P. Pouget, *Eur. Phys. J. B* **20**, 321 (2001).

- ¹⁹A. Akrap, A. Rudolf, F. Rullier-Albenque, H. Berger, and L. Forró, *Phys. Rev. B* **77**, 115142 (2008).
- ²⁰A. Gauzzi, N. Barišić, F. Licci, G. Calestani, F. Bolzoni, P. Fazekas, E. Giloili, and L. Forró, *Int. J. Mod. Phys. B* **17**, 3503 (2003).
- ²¹S. Bernu, P. Foury-Leylekian, P. Fertey, F. Licci, A. Gauzzi, A. Akrap, H. Berger, L. Forró, and J.-P. Pouget, *Eur. Phys. Lett.* **89**, 27006 (2010).
- ²²F. Lechermann, S. Biermann, and A. Georges, *Phys. Rev. B* **76**, 085101 (2007).
- ²³The orthorhombic symmetry lowering induces a very large hybridization term between the dz^2 and Eg_1 orbitals. See Table III in Ref. 22 showing the establishment in the orthorhombic phase of a large hopping integral between A_{1g} and Eg_1 Wannier orbitals along $c/2$ V near neighbors.
- ²⁴D. Grieger, L. Boehnke, and F. Lechermann, *J. Phys.: Condens. Matter* **22**, 275601 (2010).
- ²⁵A. Akrap, V. Stevanović, M. Herak, M. Miljak, N. Barišić, H. Berger, and L. Forró, *Phys. Rev. B* **78**, 235111 (2008), and earlier references therein.
- ²⁶J. Kelber, A. H. Reis, A. T. Aldred, M. H. Mueller, O. Massenet, G. Despaquali, and G. Stucky, *J. Solid State Chem.* **30**, 357 (1979).
- ²⁷Y. Ono, *J. Phys. Soc. Jpn.* **41**, 817 (1976).
- ²⁸In the calculation performed in Ref. 27 where the filling of an isolated single band is varied, the uniform dimerized Peierls ground state cannot be kept as soon as $2k_F$ deviates from $\frac{1}{2}$ because a soliton lattice is thus formed. However, if the Peierls system is connected to a reservoir allowing it to adjust the band filling, the dimerized Peierls ground state can be stabilized for a sizeable range of chemical potential. In this situation, the phase diagram obtained in Ref. 27 remains valid. The same phase diagram is found for the spin-Peierls chain subjected to a magnetic field, which acts as a chemical potential changing the number of pseudofermions.
- ²⁹Here one assumes that the fourth-order umklapp potential of $BaVS_3$ has qualitatively the same effect as the second-order umklapp potential considered in Ref. 27. However, the energy gain for a commensurability 4 is much smaller than for a commensurability 2 (see Ref. 30).
- ³⁰A. Kotani and I. Harada, *J. Phys. Soc. Jpn.* **49**, 535 (1980).
- ³¹The amplitude of the Fourier components of the lattice displacement corresponding to a soliton-like Peierls distortion close to the commensurability 4 has been calculated in Ref. 30. It is found that the first harmonic due to the soliton lattice is smaller than the harmonic 2 of the C modulation by a factor $\pi/2$. The amplitude of the V displacement corresponding to this latter harmonic is already a factor 3 times smaller than the amplitude of the $2k_F$ primary C distortion of $BaVS_3$.³² As the satellite intensity is the square of the V displacement, one expects, for a regular soliton lattice, first harmonic reflections ~ 20 times less intense than $2k_F$ C reflections. Even in absence of disorder, these harmonics should be very hardly detectable.
- ³²S. Fagot, P. Foury-Leylekian, S. Ravy, J.-P. Pouget, M. Anne, G. Popov, M. V. Lobavov, and M. Greenblatt, *Solid State Sci.* **7**, 718 (2005).
- ³³S. Fagot, P. Foury-Leylekian, S. Ravy, J.-P. Pouget, E. Lorenzo, Y. Joly, M. Greenblatt, M. V. Lobavov, and G. Popov, *Phys. Rev. B* **73**, 033102 (2006).
- ³⁴ $T_N = 31$ K at P_{atm} does not vary appreciably under pressure until 1 GPa, the highest pressure measured (result quoted in Ref. 10).